Carbene–Carbene Interconversion between 1- and 3-Phenyl-2-propynylidenes

Masaki Noro, Takeshi Masuda, Andrew S. Ichimura, Noboru Koga, and Hiizu Iwamura*

Contribution from the Department of Chemistry, Graduate School of Science, The University of Tokyo, Hongo 7-3-1, Bunkyo-ku, Tokyo 113, Japan

Received January 28, 1994®

Abstract: 1-Phenyl-3-diazopropyne (**1d**) and 3-phenyl-3-diazopropyne (**2d**) were prepared and photolyzed under various conditions. In ethanol at ambient temperatures, both **1d** and **2d** gave a 1:10 ± 1 mixture of 1-phenyl-3-ethoxypropyne (**3**) and 3-phenyl-3-ethoxypropyne (**4**). The photolyses of matrix-isolated **1d** and **2d** at cryogenic temperatures were followed by EPR, IR, and UV–visible spectroscopy. EPR experiments in 2-methyltetrahydrofuran (MTHF), isopentane, and ethanol-d_6 matrices at 9 K showed spectra due to a mixture of the corresponding triplet carbenes **1c** ($|D/hc| = 0.543$ and $|E/hc| = 0.003$ cm^{-1}) and **2c** ($|D/hc| = 0.526$ and $|E/hc| = 0.010$ cm^{-1}). The ratio of the generated carbenes carried the memory of the starting diazo compounds; **1c** and **2c** were produced mainly from **1d** and **2d**, respectively. Carbene **2c** isomerized to **1c** at 70–90 K in MTHF and ethanol-d_6 and at 44–68 K in isopentane, indicating that **1c** was thermodynamically more stable than **2c** on the triplet ground-state potential energy surface. IR and UV–visible absorption experiments employing various media (argon, isopentane, N_2, CO/Ar, O_2/N_2, and O_2/Ar) revealed that the photolysis of **2d** afforded mostly absorptions due to **2c**. Photolysis of **1d** produced similar spectra, due mainly to **2c**, together with weak absorptions due to **1c**. The different results observed in EPR and IR experiments were explained by the difference in the matrices in which the diazo groups were photolyzed. Calculations at the ab initio MP2/DZV(d) level of theory showed that the triplet ground state of **1c** was more thermodynamically stable than **2c** by 1.41 kcal/mol, in agreement with the experimental results. The situation is reversed in the singlet manifold, where **2c** was computed to be much lower in energy than **1c**. The energy differences (ΔE_{ST}) between the singlet and triplet states were computed to be 15.7 and 11.0 kcal/mol for **1c** and **2c**, respectively, with the DZV(d) basis set.

In the course of our study on the preparation and characterization of the magnetic properties of π-conjugated polymers having radical centers on every monomer unit as side-chain pendants,[1,2] we encountered poly(diacetylene)s,[3] which can be obtained by topochemically controlled solid-state polymerization under heat, UV light, and γ-ray irradiation.[4] In these polymerizations of spatially ordered monomers, the 2-propynylidene unit is considered as an important reactive intermediate and a defect in the polymer samples. In order to obtain further insight into this polymerization mechanism, we investigated intramolecular carbene–carbene rearrangements of 2-propynylidenes.[5] There are a number of precedents for the rearrangement of the carbenes adjacent to a phenyl ring,[6] carbonyl group,[7] and double bond,[8] but less work has been reported on carbenes adjacent to triple bonds.[9] The simplest molecule in this category, 2-propynylidene, is reported to have a triplet ground state with a very low barrier to interconversion,

$$HC{\equiv}C{-}{}^{\bullet}C{}^{\bullet}{-}H \leftrightarrow HC^{\bullet}{=}C{=}{}^{\bullet}CH \leftrightarrow H{-}{}^{\bullet}C{}^{\bullet}{-}C{\equiv}CH$$

close to the vibrational energy of the ground state.[9b] Padwa and co-workers reported that thermolysis of the 3-(1-aziridinylimino) derivative of 1-phenylpropyne as a carbene precursor afforded a 2:3 mixture of ethers **3′** and **4′** in methanol.[10] Previously, we communicated the preparation of a model dimer compound, 1,8-diphenyl-1,8-bis(diazo)-4-octene-2,6-diyne (BDEC),[5a] which was photolyzed in 2-methyltetrahydrofuran (MTHF) at cryogenic temperatures to give 1-phenyl-1,3-butadiyne in 70% yield (Scheme 1). The observed cleavage reaction path could be considered as a reverse reaction of the initiation step in the solid-state polymerization of 1-phenyl-1,3-butadiyne.

In this paper we discuss the interconversion of (phenylethynyl)-carbenes **1c** and **2c** shown in Scheme 2 as studied by photoproduct analysis, EPR, IR, and UV–visible spectroscopy as well as by MO theoretical computations.

Methods and Results

Preparations of 1-Phenyldiazopropyne (1d) and 3-Phenyldiazopropyne (2d). Ethynyldiazo compounds **1d** and **2d** as precursors of carbenes **1c** and **2c** were prepared by a sequence

* Abstract published in *Advance ACS Abstracts,* June 1, 1994.

(1) Iwamura, H. *Nippon Kagaku Kaishi* (in Japanese) **1987**, 595. Iwamura, H. *Adv. Phys. Org. Chem.* **1990**, *26*, 179. Fujii, A.; Ishida, T.; Koga, N.; Iwamura, H. *Macromolecules* **1991**, *24*, 1077. Iwamura, H. *Pure Appl. Chem.* **1993**, *65*, 57.

(2) Ovchinnikov, A. A. *Theor. Chim. Acta* **1978**, *47*, 297. Tyutyulkov, N.; Schuster, P.; Polansky, P. *Theor. Chim. Acta* **1983**, *63*, 291. Nishide, H.; Yoshioka, N.; Inagaki, K.; Tsuchida, E. *Macromolecules* **1988**, *21*, 3119.

(3) Inoue, K.; Koga, N.; Iwamura, H. *J. Am. Chem. Soc.* **1991**, *113*, 9803. Iwamura, H.; Sasaki, S.; Sasagawa, N.; Inoue, K.; Koga, N. In *Magnetic Molecular Materials*; Gatteschi, D., Kahn, O., Miller, J. S., Palacio, F., Eds.; Kluwer Academic Publishers: Dordrecht, 1991; pp 53–66.

(4) Wegner, G. Z. *Pure Appl. Chem.* **1977**, *49*, 443. Baughman, R. H. *J. Appl. Phys.* **1972**, *43*, 4362. Eichele, H.; Schwoerer, M.; Huber, R.; Bloor, D. *Chem. Phys. Lett.* **1976**, *42*, 342. Sixl, H.; Newman, W.; Huber, R.; Denner, V.; Sigmund, E. *Phys. Rev. B* **1985**, *31*, 142. Sixl, H.; Mathes, R.; Schupp, A.; Ulrich, K.; Huber, R. *Chem. Phys.* **1986**, *107*, 105.

(5) (a) A preliminary account of the EPR studies appeared in: Koga, N.; Matsumura, M.; Noro, M.; Iwamura, H. *Chem. Lett.* **1991**, 1357. (b) Noro, M.; Koga, N.; Iwamura, H. *J. Am. Chem. Soc.* **1993**, *115*, 4916.

(6) (a) Jones, W. M. In *Rearrangements in Ground and Excited States*; Mayo, P. D., Ed.; Academic Press: New York, 1980; Vol. 1, Chapter 3. (b) McMahon, R. J.; Abelt, C. J.; Chapman, O. L.; Johnson, J. W.; Kreil, C. L.; Leroux, J.; Mooring, A. M.; West, P. R. *J. Am. Chem. Soc.* **1987**, *109*, 2456.

(7) Murata, S.; Yamamoto, S.; Tomioka, H. *J. Am. Chem. Soc.* **1993**, *115*, 4013. Lewars, E. J. *Chem. Rev.* **1983**, *83*, 519.

(8) York, E. J.; Dittmer, W.; Stevenson, J. R.; Bergman, R. G. *J. Am. Chem. Soc.* **1973**, *95*, 5680.

(9) (a) Bernheim, R. A.; Kempf, R. J.; Gramas, J. V.; Skell, P. S. *J. Chem. Phys.* **1965**, *43*, 196. (b) Maier, G.; Reisenauer, H. P.; Schwab, W.; Carsky, P.; Spirko, V.; Hess, B. A., Jr.; Schaad, L. J. *J. Chem. Phys.* **1989**, *91*, 4763. (c) DePinto, J. T.; McMahon, R. J. 11th IUPAC Conference on Physical Organic Chemistry, August 2–7, 1992, Ithaca, New York, Abstract B-6. (d) Shim, S. C.; Lee, T. S. *J. Org. Chem.* **1988**, *53*, 2410. (e) DePinto, J. T.; McMahon, R. J. *J. Am. Chem. Soc.* **1993**, *115*, 12573. (f) Sander, W.; Bucher, G.; Wierlacher, S. *Chem. Rev.* **1993**, *93*, 1583.

(10) Padwa, A.; Gareau, Y.; Xu, S. L. *Tetradhedron Lett.* **1991**, *32*, 983. Padwa, A.; Austin, D. J.; Gareau, Y.; Kassir, J. M.; Xu, S. L. *J. Am. Chem. Soc.* **1993**, *115*, 2637.

0002-7863/94/1516-6179$04.50/0

Scheme 1

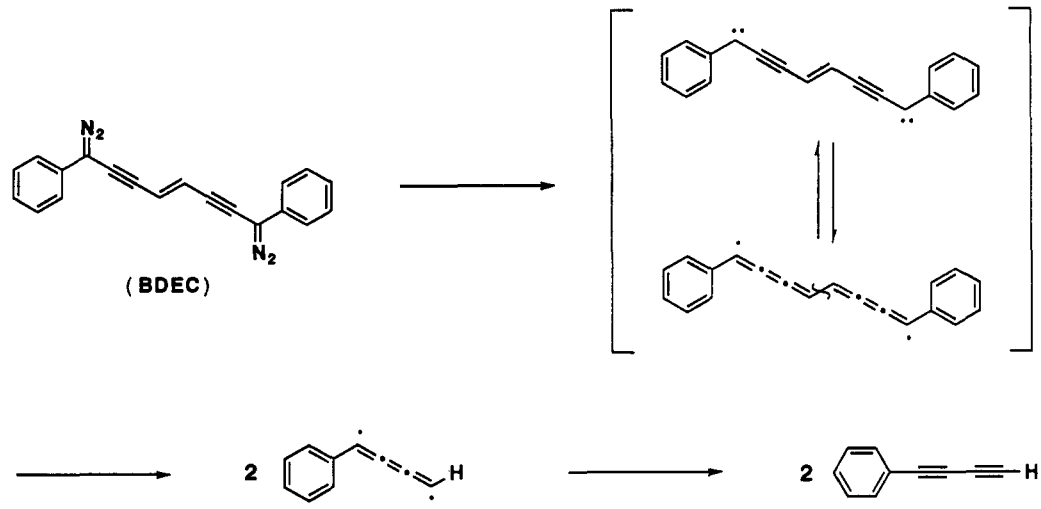

Scheme 2

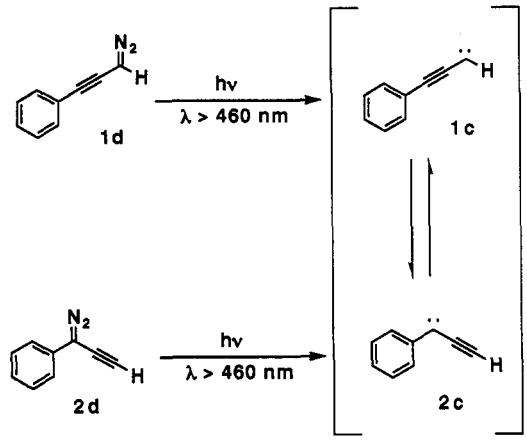

of reactions shown in Scheme 3. Amino derivatives **ms** were reacted with acetyl chloride in the presence of triethylamine, followed by treatment with nitrosonium tetrafluoroborate in dry pyridine to afford the *N*-nitrosoacetamide derivatives **mn** in quantitative yields. An alkali decomposition of **mn** with NaOH/MeOH gave crude ethynyldiazo compounds **md**. Purification of **1d** and **2d** was performed by column chromatography on basic alumina to give analytically pure red oils. The monodeuterated **D1d** was also prepared from 1-phenyl-3,3-dideuterio-3-hydroxypropyne by a similar method.

The reagents were stocked in the stage of the nitrosoacetamides, and the diazo compounds were used for spectral measurements immediately after preparation and purification. In the UV–visible spectra of **1d** and **2d** in pentane solution at ambient temperature, two characteristic absorption bands due to the diazo chromophores were observed at 296 (π–π^*) and 476 (n–π^*) nm for **1d** and at 280 (π–π^*) and 524 (n–π^*) nm for **2d**. Photolysis of the diazo compounds was carried out using the long-wavelength edge (λ > 460 nm) of the UV–visible absorptions.

Product Analysis after Photolysis of 1d and 2d. When a solution (1.5 mM) of **1d** in ethanol was irradiated (λ > 460 nm) for 60 min at 25 °C under nitrogen, the OH-insertion products 1-phenyl-3-ethoxypropyne (**3**) and 3-phenyl-3-ethoxypropyne (**4**) were obtained in a ratio of 1:9.6 in 86% overall yield. Irradiation of **2d** under similar conditions gave a 1:10.1 mixture of **3** and **4**. Photolysis of **2d** in frozen ethanol (1.3 mM) at 77 K followed by workup at room temperature gave a complex mixture. Its ^{1}H NMR spectra contained neither the signals of ethers **3** and **4** nor those of C–H insertion products, 3- and 5-phenyl-4-pentyn-2-ols. Instead, *cis*- and *trans*-1,6-diphenyl-3-hexene-1,5-diynes (**5** and **6**) were observed in ca. 20% yield. Photoproducts **3**–**6** were confirmed by ^{1}H NMR spectroscopy after their isolation from the reaction mixture by gel permeation chromatography. The authentic samples for **4** and **6** were prepared independently.

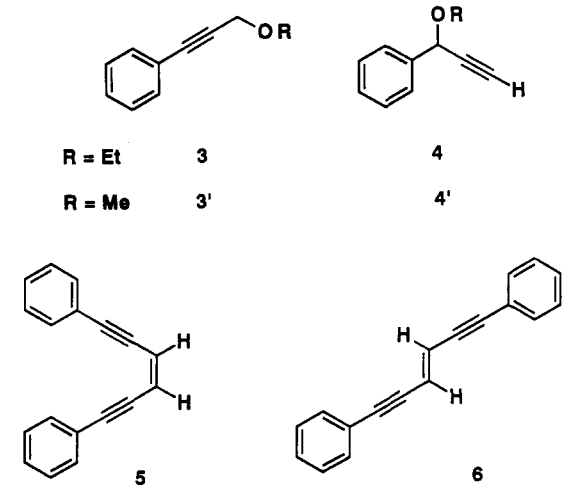

EPR Measurements. Photolyses of **1d** and **2d** in MTHF, isopentane, or ethanol-d_6 were carried out in an EPR cavity at cryogenic temperatures and followed by EPR spectroscopy. When a solid solution of **2d** in MTHF was irradiated (λ > 460 nm) at 9 K, two sets of signals due to triplet carbenes (in Figure 1c) appeared. The magnetic fields (**H**) of the Z, Y, X, and low-field Z transitions of the carbene generated in the greatest proportion gave g = 2.0031 and zero-field splitting (zfs) parameters $|D/hc|$ = 0.526 and $|E/hc|$ = 0.010 cm^{-1}. As the temperature was raised, the triplet signal intensity decreased in accordance with Curie's law up until 68 K. In the temperature range 70–90 K, the shape of the carbene signals gradually changed.

In the spectrum obtained at 9 K after recooling from 90 K (Figure 1b), the H_{-z} and H_z resonances had moved from 224.5 and 899.1 mT to 245.8 and 920.2 mT, respectively, indicating that the $|D|$ value had increased. The X and Y transitions shifted toward the center of the spectrum and sharpened, showing a decrease in the $|E|$ value; g = 2.0032, $|D/hc|$ = 0.543, and $|E/hc|$ = 0.003 cm^{-1} for the spectrum in Figure 1b. From the comparison of the zfs values as described in the Discussion section, the main components responsible for the spectra of Figure 1b and c were assigned to carbenes **1c** and **2c**, respectively. The temperature dependences of the intensities (I) of the H_{-z} transitions at 224.5 and 245.8 mT representing an approximate measure of the relative amounts of **2c** and **1c** after the photolysis of **2d** in an isopentane

Scheme 3

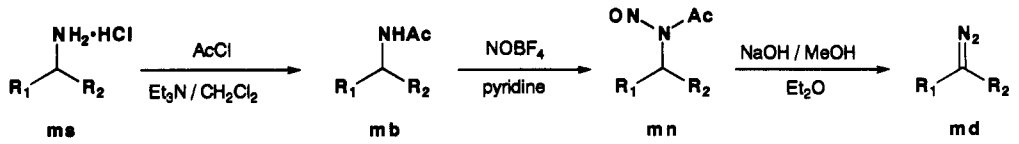

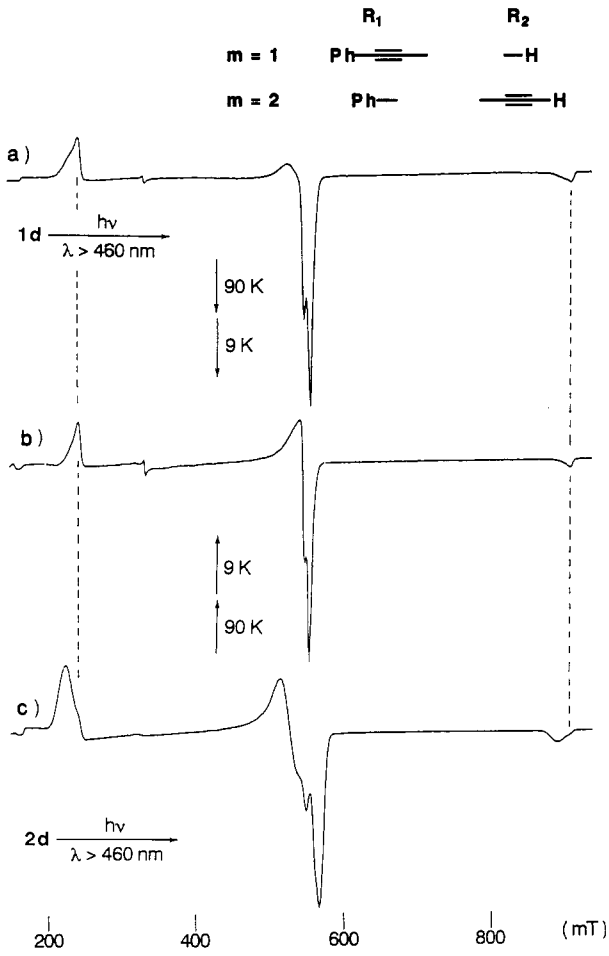

Figure 1. X-band (ν = 9.483 GHz) EPR spectra in MTHF matrices at 9 K (a) and (c) after photolysis of **1d** and **2d**, respectively, and (b) after annealing of spectra a and c at 90 K and recooling to 9 K.

matrix are given as IT vs T plots in Figure 2. If there were no change in the amount of either triplet species, the Curie law indicates that such a plot should consist of a horizontal lines. The increase of **1c** at the expense of **2c** at temperatures higher than 44 K is clearly indicated. The ratio of the formation of the two carbenes depended on the kind of matrices and wavelength of irradiating light; the **1c**/**2c** ratios decreased in the order ethanol-d_6 ~ isopentane > MTHF and increased by use of shorter wavelength irradiation ($\lambda > 320$ nm). However, once the carbenes were generated, additional shorter wavelength irradiation did not change the EPR spectra significantly. The temperatures at which rearrangement from **2c** to **1c** began were found to be 44 K in isopentane and 70 K in EtOH-d_6 and MTHF matrices.

Ethynyldiazo compound **1d** was irradiated under similar conditions to give an EPR spectrum (Figure 1a) containing mainly the signals assigned to carbene **1c**. The signals due to a small amount of carbene **2c** were also noted. After annealing at 80–90 K, the spectrum changed from that in Figure 1a to that in Figure 1b. Neither increase in the major signals due to carbene **1c** nor decrease in the minor signals of **2c** was so obvious as in the spectral change observed for **2d** in the rearranging temperature region (Figure 2). The decomposition of ethynylcarbene **1c** in ethanol-d_6 and isopentane at higher temperatures accompanied the formation of a new triplet diradical with zfs parameters $|D/hc| = 0.012$ and $|E/hc| = 0$ cm^{-1}.

Infrared Spectra in Argon Matrices. Diazo compounds **1d** and **2d** were photolyzed ($\lambda > 460$ nm) at 14 K. The strong absorptions due to the C≡C and C=N$^+$=N$^-$ bonds at 2212 and 2071 cm^{-1} for **1d** (Figure 3a) and at 2120 and 2060 cm^{-1} for **2d** (Figure 3d), respectively, disappeared efficiently. Absorptions characteristic of C(=N$_2$)—H stretching at 3092 cm^{-1} in **1d** and ≡C—H stretching at 3321 cm^{-1} in **2d** also disappeared. The spectra obtained upon irradiation of **1d** and **2d** for 800 min (Figure 3b and c, respectively) were very similar to each other and had absorptions at 3278 and 2147 cm^{-1} assigned to ≡C—H and C≡C stretches, respectively. Phenyl C–H out-of-plane deformation bands at ca. 690 and 750 cm^{-1} both in **1d** and in **2d** shifted to 678 and 747 cm^{-1} in Figure 3c and further split into two pairs at 678 (strong) and 690 (weak) and 747 (s) and 756 (w) cm^{-1} in Figure 3b.

After annealing at 33 K, no significant changes in the spectra from **2d** were observed (Figure 3c), whereas the absorptions at 3278, 747, and 678 cm^{-1} in the spectra from **1d** disappeared and new absorptions appeared at ca. 3300 cm^{-1} and below 1000 cm^{-1} in addition to the ones at 690 and 756 cm^{-1}.

When deuterated compound **D1d** was photolyzed under similar conditions, the absorptions at 2189 and 2071 cm^{-1} assigned to C—D and C=N$^+$=N$^-$ stretching, respectively, disappeared, and a new absorption at 2474 cm^{-1} due to terminal ≡C—D stretching appeared. An absorption at 2211 cm^{-1} due to C≡C stretching also disappeared, and a new one at 2146 cm^{-1} appeared after photolysis. This shift in the C≡C stretch was close to the one observed after the photolysis of **1d** under similar conditions. The origin of this new absorption at 2146 cm^{-1} will be discussed in a later section. However, neither -•C•—H nor -•C•—D stretching modes for **1c** or **D1c** were identified.

Infrared Spectra in Isopentane Solid Solutions. Ethynyldiazo compounds **1d** and **2d** were irradiated ($\lambda > 460$ nm) for 1423 and 1050 min, respectively, in isopentane solid solution at 14 K. Before irradiation, both of the spectra were similar to those in Ar matrix except for the signals due to isopentane. When **1d** in isopentane matrix was irradiated, the spectrum (Figure 4b) showed two pairs of new absorptions at 678 and 747 cm^{-1} (B) and at 690 and 758 cm^{-1} (A) in the phenyl C–H out-of-plane deformation region. Subsequently, as the temperature was raised above 65 K, the absorbances at 690 and 758 cm^{-1} (A) increased slightly. The latter bands marked A in Figure 4c remained even at 100 K.

IR Spectra in Argon Containing CO. Irradiation ($\lambda > 460$ nm) of **1d** in CO-doped argon (10.3% of CO in Ar) at 14 K for 800 min gave an IR spectrum similar to that obtained in neat Ar matrix. In this case, the signal due to ≡C—H stretching appeared at 3265 cm^{-1}. After annealing at 36 K, the spectrum changed completely, indicating that the generated carbene had reacted with CO. However, the absorptions expected for a ketene could not be observed under various conditions of CO concentration (0.4–10.3%) and temperature. If a ketene was generated under these conditions, its C=C=O stretching absorption might

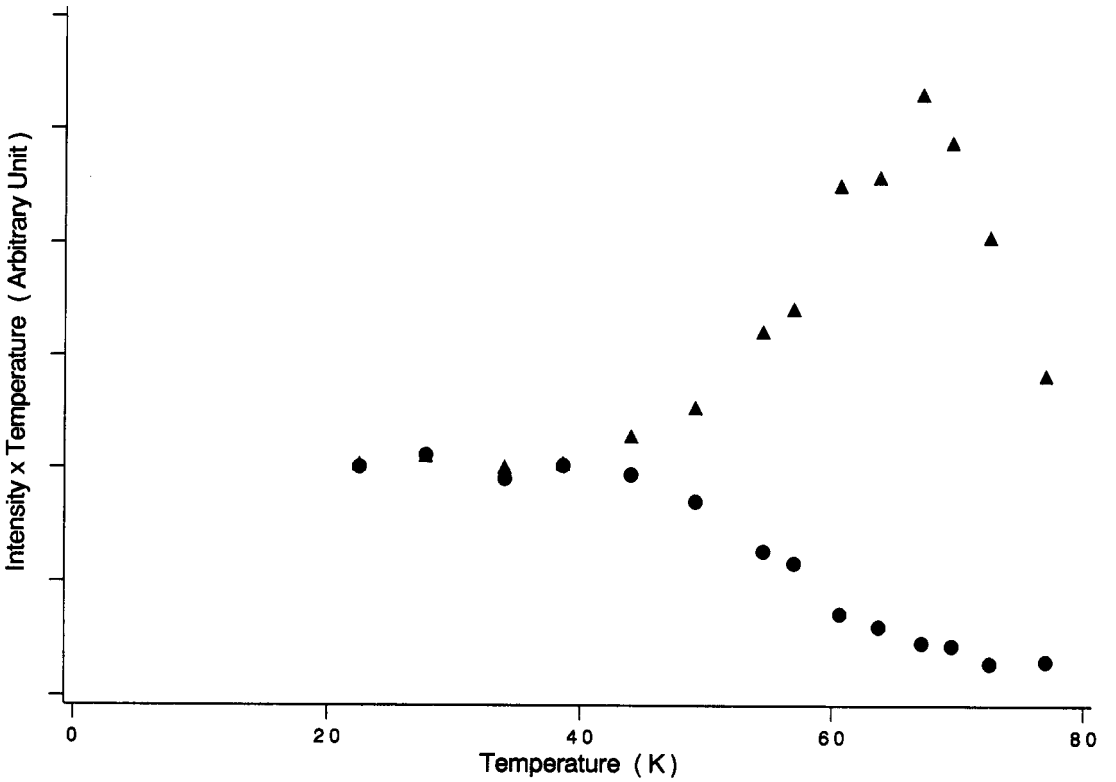

Figure 2. Temperature dependence of the intensities of EPR signals at 234.4 (●) and 246.2 mT (▲) after photolysis of **2d** in isopentane matrix.

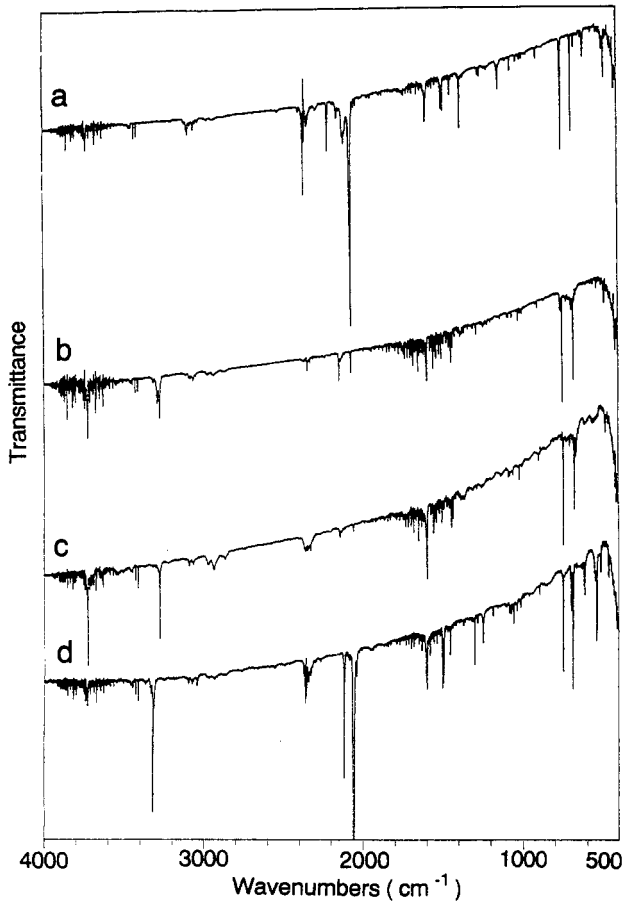

Figure 3. IR spectra of (a) **1d** and (d) **2d** in argon matrix at 14 K; (b) and (c) those after irradiation ($\lambda > 460$ nm), respectively.

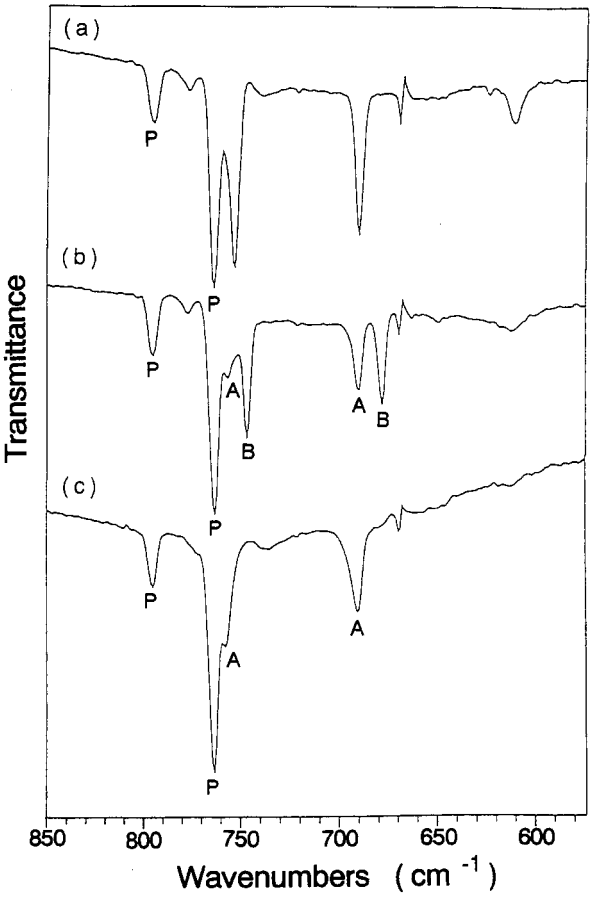

Figure 4. IR spectra of **1d** in isopentane solid solution at 14 K (a) before irradiation, (b) after irradiation ($\lambda > 460$ nm), and (c) followed by raising the temperature at 80 K. Absorptions marked P are due to isopentane.

have been buried under the strong absorption due to free CO (2139 cm^{-1}).

IR Spectra in O_2-Doped Argon Matrices. Photolysis of **1d** and **2d** in argon matrices containing 0.46, 5.0, and 18.7% oxygen and

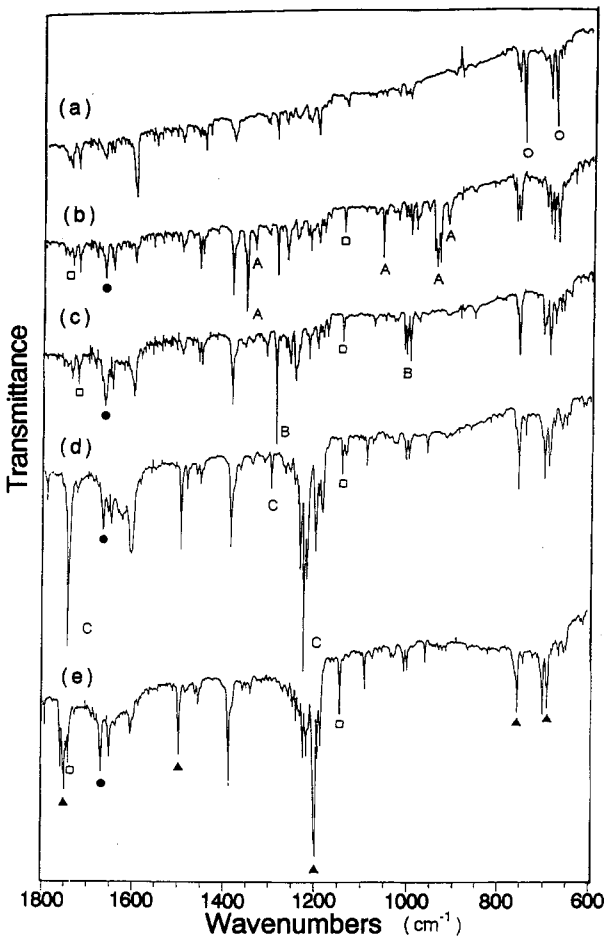

Figure 5. IR spectra of **1d** in 0.46% O_2-doped argon matrices (a) after irradiation ($\lambda > 460$ nm) at 13 K, followed by (b) annealing at 40 K and recooling at 13 K, (c) further irradiation ($\lambda > 600$ nm), (d) further irradiation ($\lambda > 350$ nm), and (e) annealing at 40 K and recooling at 13 K. Absorptions A and B are assigned to **8** and **9**, respectively. Absorptions marked O, □, ●, and ▲ are due to **2c**, **1a**, **2k**, and **7**, respectively.

subsequent photoreactions of O_2-trapped products were followed by IR spectroscopy. The IR spectral changes of **1d** in the region 1800–600 cm^{-1} are represented in Figure 5. Irradiation of **1d** ($\lambda > 460$ nm) for 780 min at 13 K in 0.46% O_2-doped Ar matrix gave an IR spectrum (Figure 5a) consisting of absorptions similar to those of Figure 3b or c. Additional weak absorptions for **2k** at 3311, 2109, and 1666 cm^{-1} due to an O_2-trapped product were observed. After the temperature was raised to 40 K to allow for the complete reaction with oxygen and then recooled to 12 K, the absorptions at 678 and 747 cm^{-1} disappeared completely, and new absorptions marked as A and **1a** at 3534, 2251, 2229, 2222, 1738, and 1142 cm^{-1} appeared, as shown in Figure 5b. Subsequent longer wavelength irradiation ($\lambda > 600$ nm) caused the increase in the absorptivity of ketone **2k** and the appearance of absorptions B at the expense of A (Figure 5c). By shorter wavelength irradiation ($\lambda > 350$ nm), absorptions B changed to C (Figure 5d) and then finally to **7** (Figure 5e) after an annealing–cooling cycle. Final product **7** has absorptions at 3307, 2136, 1748, 1495, 1197, 754, and 690 cm^{-1}. The O_2-trapped products, **1a**, **2k**, and **7**, were assigned to phenylpropiolic acid, ethynyl phenyl ketone, and phenyl propiolate, respectively, by the comparison of their IR spectra with those of the authentic samples prepared independently. The absorptions A and B were identified as carbonyl oxide **8** and dioxirane **9**, respectively, by comparison with those in the literature.[11] A photoproduct having absorptions C was postulated to be an intermediate between dioxirane **9** and migration product **7**. The increase in the O_2 concentration resulted in the formation of a larger amount of ketone **2k** directly after the photolysis of **1d**. When **1d** in 18.7% O_2-doped Ar was irradiated, the spectrum in Figure 5c was directly obtained without observation of spectra in Figure 5a and b. Ozone (1030 cm^{-1}) and ketone **2k** were also observed. Even under these conditions of large O_2 concentration, aldehyde **1f**, which corresponds to **2k** from **2c**, was not detected.

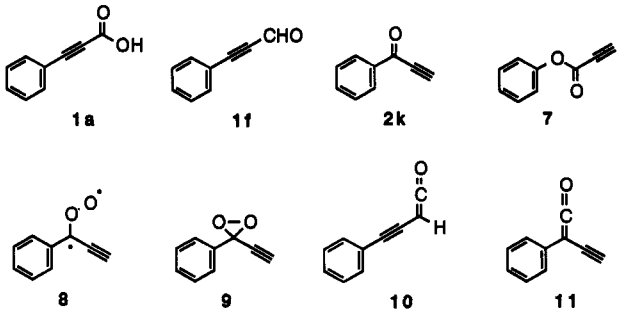

The photolysis of **2d** under a similar sequence of irradiations and temperature conditions gave essentially the same spectra as those from **1d** except for the absence of the absorptions due to carboxylic acid **1a**.

UV–Visible Spectra in Argon and Nitrogen Matrices. Photolysis of diazo compounds **1d** and **2d** at 14 K in argon matrix was monitored by UV–visible absorption spectroscopy. When either **1d** or **2d** was irradiated ($\lambda > 460$ nm), new absorptions at 268 and 292 nm (see Figure 6a in N_2 matrix) appeared at the expense of the π–π^* absorption band of the α-diazobenzyl chromophore with isosbestic points at 272 for **1d** and 251, 272, and 295 nm for **2d**. The 1-h irradiation of **1d** and **2d** gave new absorptions which were similar to each other. The changes in the UV–visible spectra after the photolysis of **1d** in O_2-doped nitrogen (0.5% of O_2 in N_2) followed by annealing are reproduced in Figure 6. After annealing at 34 K, the new absorption disappeared and a broad band with a maximum at 414 nm appeared, as shown in spectra a and b (Figure 6). By long-wavelength irradiation ($\lambda > 600$ nm), spectrum b disappeared to give spectrum c. The observed new spectrum a and a broad absorption in spectrum b were assigned to the carbene and carbonyl oxide **5**, respectively, by comparison with those spectra in the literature.[11,12] Spectrum b of O_2 adduct **5** disappeared by the formation (spectrum c) of the dioxirane **6**, as observed in the IR experiment.

Comparison of the Relative Energies of 1c and 2c by ab Initio Calculations. The relative energies of the two isomers were obtained by first optimizing the geometries of the triplet and lowest excited singlet states with a UHF and a GVB wave function, respectively. The total energies were then calculated by means of second-order perturbation theory (MP2). A basis set of double ζ[13] (DZ) quality was used in the geometry optimizations and MP2 calculations, and the split valence contraction[14] of the DZ basis augmented by a set of d functions on carbon (DZV(d)) was also used for selected MP2 calculations. The optimized geometries and relative energies are reported in Figure 7 and Table 1, respectively. Further details of the computational methodology may be found in the Experimental Section.

The triplet geometries show significant delocalization of the carbene unpaired electrons both in the ethynyl fragment and in the phenyl ring, as shown by the deviation of the carbon–carbon bond lengths from typical alkene and alkyne values. Although there is some difference in the bonding parameters of the ethynyl

(11) Ganzer, G. A.; Sheridan, R. S.; Liu, M. T. H. *J. Am. Chem. Soc.* **1986**, *108*, 1517. Sander, W. W. *J. Org. Chem.* **1988**, *53*, 121. Sander, W. W. *J. Org. Chem.* **1989**, *54*, 333.

(12) Sugawara, T.; Iwamura, H.; Hayashi, H.; Sekiguchi, A.; Ando, W.; Liu, M. T. H. *Chem. Lett.* **1983**, 1261.

(13) Dunning, T. H. *J. Chem. Phys.* **1970**, *53*, 2823.

(14) Dunning, T. H.; Hay, P. J. *Methods of Electronic Structure*; Plenum: New York, 1977; Vol. 2.

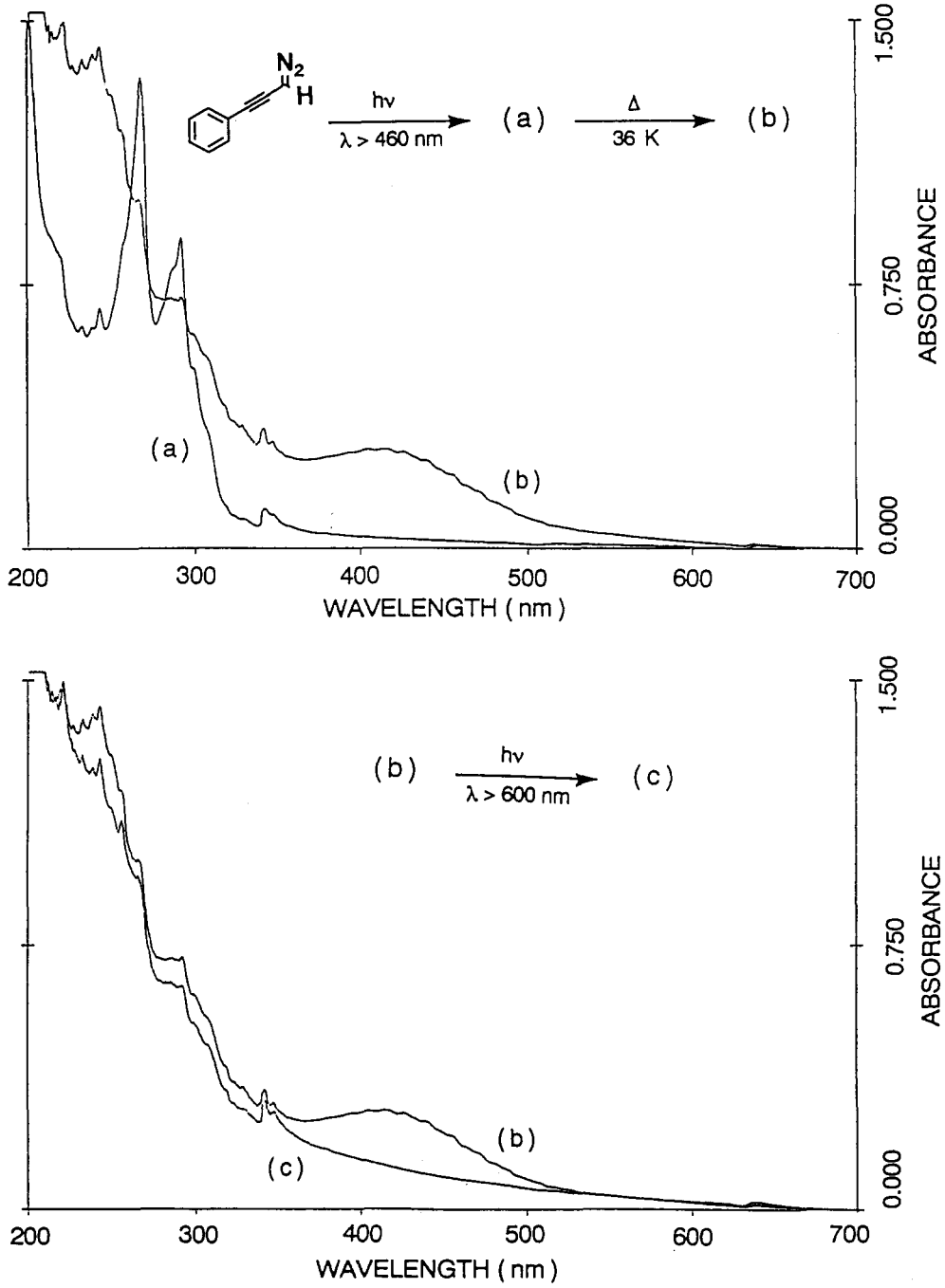

Figure 6. UV–visible spectra of **1d** in 0.5% O_2-doped nitrogen matrices after (a) irradiation ($\lambda > 460$ nm) at 14 K, (b) annealing at 34 K, and (c) reirradiation ($\lambda > 600$ nm).

portion of triplet **1c** and **2e**, which may reflect the proximity of the phenyl ring to the carbene center in **2c**, these values are nevertheless within a range found by other researchers for 2-propynylidene at the Hartree–Fock level of theory.[9b,15] The bond angles at the carbene centers of the UHF/DZ geometries were found to be 152.1° and 151.2° for **1c** and **2c**, respectively, in fair agreement with the results (157–160°) of ^{13}C-labeling studies by DePinto and McMahon.[9c] Comparing the bonding parameters of the ethynyl portions of the singlet GVB geometries to those of propynylidene, the parameters are again similar to previous studies[9b,15] except for the relatively large bond angle (120.1°) at the carbene center for singlet **2c**. For singlet 2-propynylidene, typical computed values range from 109° to 113°, and the difference may simply be due to steric repulsions with the phenyl ring.

When the energies computed with the restricted open-shell MP2 (ROMP2) wave function and the DZV(d) basis set are compared, the triplet state of **1c** was predicted to be more thermodynamically stable than **2c** by 1.41 kcal/mol. The situation is reversed in the singlet manifold, where **2c** was computed to be much lower in energy than **1c** by 3.20 kcal/mol at the MP2/DZV(d) level of theory. Hence, the computed singlet–triplet (S–T) energy differences for the two isomers are predicted to be rather different: 15.7 and 11.0 kcal/mol for **1c** and **2c**, respectively (Figure 8). The primary effect of the polarization functions was to decrease the S–T energy splitting by approximately 7 kcal/mol for both isomers: ΔE_{ST} = 22.6 and 17.7 kcal/mol for **1c** and **2c**, respectively, with the DZ basis set. In addition, the triplet and singlet states of **1c** were stabilized by approximately 1.3–1.5 kcal/mol when d functions were included in the basis set, as can be seen when the ROMP2 and MP2 energy differences between isomers **1c** and **2c** are compared (Figure 8).

(15) Defrees, D. J.; McLean, A. D. *Astrophys. J.* **1986**, *308*, L31. Jonas, V.; Bohme, M.; Frenking, G. *J. Phys. Chem.* **1992**, *96*, 1640.

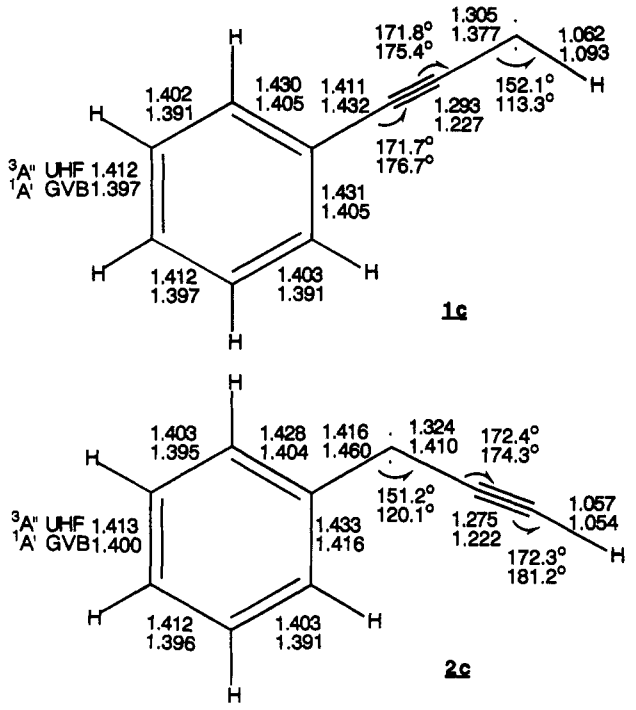

Figure 7. Geometries of singlet and triplet **1c** and **2c**.

Table 1. Calculated Total Energies (hartrees) and Relative Energies (kcal/mol) of the Triplet and Singlet **1c** and **2c**

^{3}A" UHF Geometry

	1c	2c	ΔE(1c – 2c)
	DZ Basis		
ROHF	−344.048 575	−344.053 358	3.00
UHF	−344.122 848	−344.123 382	0.34
ROMP2	−344.795 068	−344.794 859	−0.13
UMP2	−344.734 008	−344.735 579	0.99
	DZV(d) Basis		
ROHF	−344.172 069	−344.177 003	3.10
ROMP2	−345.263 531	−345.261 281	−1.41

^{1}A' GVB Geometry

	1c	2c	ΔE(1c – 2c)
	DZ Basis		
GVB	−344.056 009	−344.068 372	7.76
RHF	−344.042 666	−344.045 420	1.73
MP2	−344.759 066	−344.766 650	4.76
	DZV(d) Basis		
RHF	−344.176 525	−344.178 059	0.96
MP2	−345.238 567	−345.243 669	3.20

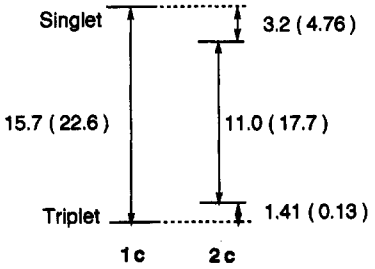

Figure 8. Comparison of the relative MP2 energies of the triplet and singlet states of **1c** and **2c** and the ΔE_{ST} in kcal/mol. The energies were computed with DZV(d) basis set (DZ basis in parentheses).

Discussion

Reactivities of 1d and 2d. Irradiation of **1d** and **2d** in ethanol at 20 °C gave OH insertion products **3** and **4** in 1:10 ± 1 ratios. The photoproducts are considered to be formed by the reaction

Scheme 4

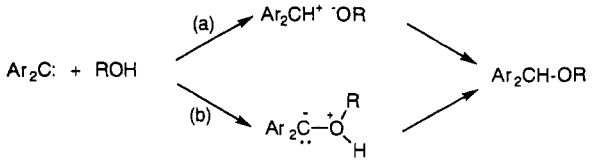

of the initially generated singlet carbenes with ethanol. Since singlet **2c** is predicted at the MP2/DZV(d) level of theory to lie below **1c** by 3.2 kcal/mol, **2c** would be more abundant if an equilibrium condition existed and the product distribution could be understood as a matter of course. However, the interconversion between **1c** and **2c** is expected to be more facile than their reactions at ambient temperature,[9] and the Curtin–Hammett principle should apply. The product distribution should be interpreted in terms of higher reactivity of **2c** than **1c**. Actually, Padwa et al. obtained the methyl ethers **3'** and **4'** in a 2:3 ratio.[10] Since the temperature used in their experiments (80 °C) was much higher than that used in the present study, their observations are interpreted as the reduced selectivity of the carbenes due mainly to the higher temperature. In isopropyl alcohol, the yield of the corresponding OH insertion products was reversed to 5:1, demonstrating that the product distributions under these conditions have nothing to do with the relative stability of the isomeric singlet carbenes **1c** and **2c**.[10]

The OH insertion reaction of a variety of singlet carbenes with alcohols has been discussed in terms of two stepwise mechanisms as described in Scheme 4.[16] In path a, a singlet carbene is protonated by an alcohol to make a carbonium ion, while in path b, a singlet carbene attacks the oxygen of an alcohol electrophilically to produce an ylide. More abundant formation of **4** relative to **3** suggests that **2c** is either more readily protonated or more electrophilic toward oxygen than **1c**. The inversion of the product ratios in isopropyl alcohol can be attributed to a steric effect of the bulkier alcohol.

A completely different set of reactions occurred after photolysis of **2d** in ethanol at 77 K. Neither the expected CH insertion products due to a triplet carbene nor the OH insertion products from a singlet carbene were obtained. Only a *cis* and *trans* mixture of **5** and **6** formally produced by the dimerization of triplet **1c** was isolated from a complex mixture of the photoproducts.

These results bring a couple of important messages. Firstly, the absence of the OH insertion products in ethanol at 77 K shows that the reaction of the singlet carbenes (Scheme 4) requires a certain amount of activation energy and cannot react with the frozen solvent before intersystem crossing to the triplets.[17] Secondly, since **2c** cannot accumulate but instead isomerizes to **1c** under these irradiation conditions as observed by EPR ($|D/hc|$ = 0.541 and $|E/hc|$ = 0.003 cm^{-1} in ethanol glass), the formation of **5** and **6** is literally interpreted as arising from dimerization of triplet **1c** at ≥77 K. Interaction between two triplet species gives rise to six nonionic electronic states in which two are singlet, three are triplet, and one is quintet. When a weak interaction between two strongly coupled triplets as in carbenes is concerned, these six states reduce to one each of singlet, triplet, and quintet states. Thus the formation of singlet recombination products is not forbidden, and a chemical reaction version of the annihilation of two excited triplet species may be operative.

Structures and Thermodynamic Stabilities of Carbenes 1c and 2c. Skell and co-workers[9a] reported the EPR spectrum of **1c** generated by photolysis of **1d** in $CFCl_3$ at 77 K. Their zfs values, $|D/hc|$ = 0.541 and $|E/hc|$ = 0.0035 cm^{-1}, are in good agreement

(16) Kirmse, W.; Kilian, J. *J. Am. Chem. Soc.* **1990**, *112*, 6399. Bethell, D.; Newall, A. R.; Stevens, G.; Whittaker, D. *J. Chem. Soc. B* **1969**, 749. Bethell, D.; Newall, A. R.; Whittaker, D. *J. Chem. Soc. B* **1971**, 23. Belt, S. T.; Bohne, C.; Charette, G.; Sugamori, S. E.; Scaiano, J. C. *J. Am. Chem. Soc.* **1993**, *115*, 2200.

(17) Tomioka, H.; Izawa, Y. *J Am. Chem. Soc.* **1977**, *99*, 6128.

with those for **1c** in this study. When the structures of the triplet carbenes **1c** and **2c** are compared (Figure 7), one would expect that the $|D|$ value of **2c** might be smaller than that of **1c**, since the $|D|$ values of carbenes are governed by the spin density on the σ- and π-orbitals at the carbene center and the latter of **2c** is located between the phenyl and ethynyl groups, allowing for greater delocalization. The zfs parameters of **2c** ($|D/hc| = 0.526$, $|E/hc| = 0.010$ cm^{-1}) are close to those of phenylcarbene ($|D/hc| = 0.515$, $|E/hc| = 0.025$ cm^{-1}),[18] suggesting that delocalization of the carbene π-spin onto the phenyl ring takes place to a greater extent than both σ- and π-spin delocalization onto the ethynyl chromophore. However, carbene **1c** must also be fairly delocalized since its D value is only slightly larger than that of **2c**. The observed E values are also in accord with qualitative expectations based on the difference in structure. Carbene **1c** is approximately axially symmetric (C_2 axis) when the nonrigidity of the propynylidene group is taken into account, while **2c** is rather bent at the carbene carbon by comparison. The CCC bending motion, which might allow for a more linear geometry, should be fairly hindered in the low-temperature matrices such that **2c** has a lower effective symmetry and its E value should be larger than that of **1c**. When the E values are compared, it appears that the ethynylcarbene part of **1c** ($|D/hc| = 0.543$, $|E/hc| = 0.003$ cm^{-1}) has a structure which is similar to 2-propynylidene ($|D/hc| = 0.628$ and $|E/hc| = 0.000$ cm^{-1}).[9b] Therefore, we conclude that the carbenes observed in Figure 1c and a correspond to **2c** and **1c**, respectively. The carbene–carbene rearrangement was observed to take place from **2c** to **1c** at 70–90 K in MTHF and ethanol-d_6 and at 44–68 K in isopentane solid solution. DePinto and McMahon also reported observing this rearrangement at 37 K in EPR experiments in argon matrices.[9c]

The change in the $|D/hc|$ values from 0.526 to 0.541 cm^{-1} during this rearrangement indicates that the reaction occurred in the direction from a more delocalized to localized unpaired electron spin or from a more highly substituted carbon to a primary carbon. The small E value of **1c** suggests but not necessarily verifies a more linearized structure with intermediate hybridization between sp and sp^2 for each carbon atom. In 2-propynylidene, ab initio calculations[9b,15] find a structure that is very delocalized, where the carbene carbon has a hybrid character which is intermediate between sp^2 and sp, but closer to sp^2, while the acetylenic carbons also have intermediate bonding character, but closer to sp. The EPR experiments suggest that having an acetylenic sp carbon rather than an sp^2 hybridized carbon adjacent to the phenyl ring is energetically favorable. This interesting finding was also observed in the analogous carbene, 1,5-diphenylpenta-2,4-diynylidene (**12c**), obtained after carbene–carbene rearrangement, which had $|D/hc| = 0.497$ and $|E/hc| < 0.001$ cm^{-1}, which implies an almost linearly symmetric geometry.[5b]

Recently, 1,3-diphenyl-2-propynylidene was found to show an apparently similar EPR spectral change on annealing, but the change accompanying a decrease in the $|D|$ value was ascribed to the structural relaxation rather than the bond replacement.[9e]

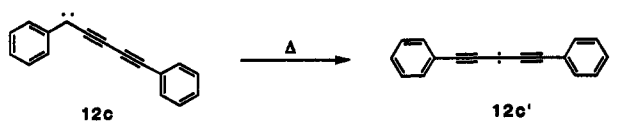

12c **12c'**

The EPR observations revealed that the formation ratio of the isomeric carbenes depended on the irradiation wavelength and the matrix media. The observed rearrangement of the triplet ground states is not photochemical but thermal, and carbene **1c** is found to be thermodynamically more stable than **2c** in organic media. The intrinsic energy barrier between **1c** and **2c** was estimated to be <133 cal/mol from the lowest rearrangement temperature, 67 K, observed in isopentane matrix.

(18) Trozzolo, A. M.; Murray, R. W.; Wasserman, E. *J Am. Chem. Soc.* **1962**, *84*, 4990.

Scheme 5

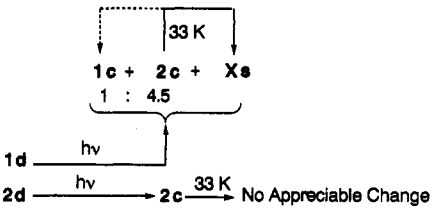

Some Comments on the IR Matrix Isolation Studies. After photolysis of both isomeric diazo compounds **1d** and **2d** in argon matrices, similar IR spectra having signals at 3278, 2147, 747, and 678 cm^{-1} were obtained. The similarity of the spectra after photolysis suggested that only **1c** or **2c** was generated from both precursors or that a mixture of **1c** and **2c** was generated in the same proportions from **1d** and **2d**.

In the spectra after photolysis of both the diazo compounds, an absorption at 3278 cm^{-1} was assigned to the acetylenic ≡C–H stretch. This absorption strongly suggests the formation of **2c** in the photolysis of **1d** and implies the existence of the corresponding C≡C bond. The absorption at 2147 cm^{-1} assigned to the C≡C stretch was also observed in the spectra but cannot be assigned to **2c** for the following reasons. In the spectrum from **1d**, this absorption did not change after annealing, although the 3278-cm^{-1} absorption and the other ones (at 747 and 678 cm^{-1}) assigned to **2c** disappeared. In addition, the 2147-cm^{-1} absorption intensity relative to other **2c** absorptions depended on whether the absorption was generated from diazo compound **1d** or **2d**. Lastly, no secondary isotope effect was observed for this acetylenic stretch since an absorption was observed at 2146 cm^{-1} after photolysis of **D1d** (C≡C stretch 2211 cm^{-1}). From these considerations, it is concluded that the observed absorption at 2147 cm^{-1} was not due to **2c** but to unidentified compounds, X, and the absorption due to the C≡C stretch for **2c** was too weak to be detected.

After complete photolysis of **1d** in argon matrix, the two absorptions at 752 and 690 cm^{-1} were split into 758, 747 cm^{-1} and 690, 678 cm^{-1}, while the corresponding signals at 748 and 690 cm^{-1} of **2d** shifted to 747 and 678 cm^{-1}. The relative intensity of 756–747 cm^{-1} (or 690–678 cm^{-1}) in the spectrum from **1d** was media dependent; the intensity ratio of the 690–678-cm^{-1} absorptions (or 756–747 cm^{-1}) was 1:4.5 in argon and 1:1.2–1.6 in isopentane, respectively. After annealing at 33 K, the pair of absorptions at 756 and 690 cm^{-1} in the spectrum from **1d** disappeared and those at 747 and 678 cm^{-1} remained. No significant changes in the spectra suggesting the isomerization from **2c** to **1c** after annealing the argon matrices could be observed. However, when the pair of absorptions at 747 and 678 cm^{-1} disappeared above 67 K in isopentane matrix, the intensity of the bands at 758 and 690 cm^{-1} increased slightly. The former two absorptions are tentatively assigned to **2c**, and the latter two absorptions are ascribed to **1c**, since the isomerization occurs in isopentane above 67 K according to our EPR experiments. Unfortunately, at temperatures above 67 K in isopentane, the C̈—H stretch from **1c** could not be observed, nor could a definite C≡C signal be identified. Therefore, our IR experiments carried out in isopentane do not allow for conclusive identification of **1c**. Nevertheless, we feel that there is permissive evidence to conclude that one carbene **2c** is the dominant photoproduct from the irradiation of either **1d** or **2d** in argon matrix. The results of IR experiments after photolysis of both isomeric diazo **1d** and **2d** in argon matrices are summarized in Scheme 5.

In IR experiments in argon and isopentane, rearrangement of **1c** to **2c** directly after photolysis was clearly observed, but the thermal one from **2c** to **1c** is still indistinct. As described in Scheme 5, after annealing the argon matrices at 33 K, the spectrum obtained by photolysis of **2d** shows essentially no change, while rearranged carbene **2c** obtained by photolysis of **1d** was mainly

Scheme 6

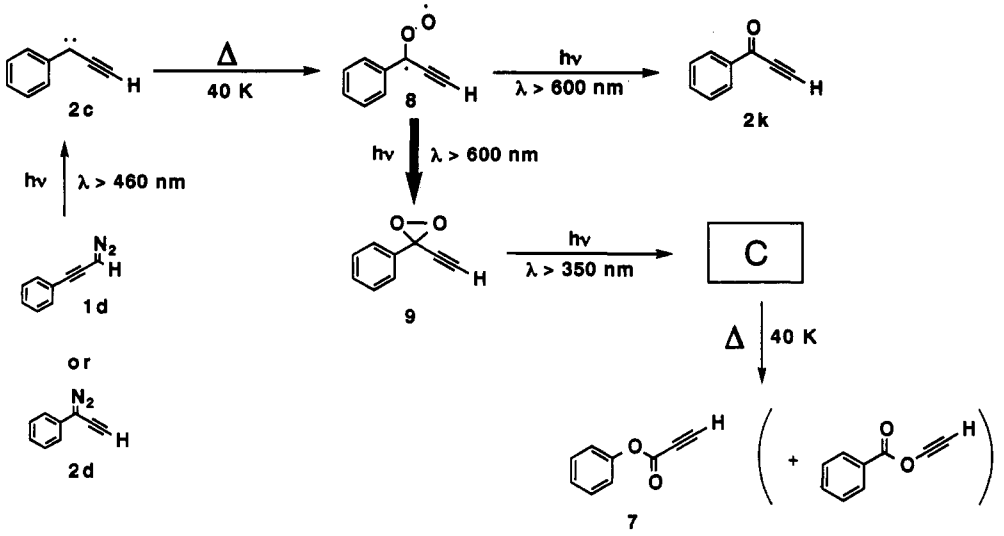

converted to unidentified compounds **X**. Even in the isopentane matrix, the decrease of **2c** did not correspond to the increase of **1c**. The difference in behavior of **2c** from **1d** and **2d** may be caused by the large conformation change in going from **1c** to **2c**, which alters the structure of the argon matrix surrounding the carbene. Thus, the rearranged **2c** from **1d** has a degree of freedom permitting further rearrangement, which **2c** from **2d** does not have because the latter process does not require a large conformational change.

The photolyses of **1d** and **2d** isolated in an argon matrix containing various amounts of CO or O_2 at 14 K were followed by IR measurements. In the CO-trapping experiment, detection of ketene **10** or **11** was unsuccessful, but any formation of **10** or **11** might have been masked by the free CO band. On the other hand, a weak absorption due to carboxylic acid **1a** was detected after photolysis of **1d** but not when **2d** was photolyzed in O_2-trapping experiments, indicating that a small amount of **1c** was generated by the photolysis of the corresponding diazo **1d** and not from **2d** under similar conditions. This observation clearly revealed that the rearrangement from **1c** to **2c** by photolysis was the main event and that rearrangement in the reverse direction was disadvantageous under these conditions. The reactions with O_2 are summarized in Scheme 6.

Similar UV–visible spectra in the argon matrix were obtained by the photolysis of the two isomeric diazo compounds, **1d** and **2d**. In the O_2-doped nitrogen matrix, an absorption due to carbonyl oxide was observed which disappeared after irradiation at longer wavelengths ($\lambda > 600$ nm). These results are consistent with the IR experiments and support our conclusion that the one carbene was predominantly generated under these conditions.

Comparison of Theory and Experiment. In argon matrices, only one triplet isomer, **2c**, was observed after photolysis of both diazo compounds. This suggests that before relaxation of the singlet state to the ground state occurs, the isomerization takes place to the lower energy singlet carbene, whose potential well is sufficiently deep to prevent the reverse process. Calculations at the MP2/DZV(d) level predict that singlet **2c** is much lower than **1c** by 3.20 kcal/mol. Whether or not the isomerization occurs will depend on the height of the barrier to interconversion and was shown in this study to depend on the type of matrix used (see discussion below). The relative stability of singlet carbenes has been shown by a number of ab initio studies[19] to be due to the ability of a substituent to donate a pair of electrons to the vacant p-type orbital of the singlet state. The carbene center in **2c** is connected to two π-donating substituents, phenyl and ethynyl, which can stabilize the singlet state. **1c** has only one substituent capable of π-electron donation, and therefore its singlet state should be higher in energy than that of **2c**, as predicted.

While experimental and theoretical evidence exists showing how electron donation stabilizes the singlet state, the factors controlling the stability of the triplet state are much less clear. However, it is not unreasonable to suppose that **2c** would experience greater steric repulsion than **1c**, and so if the carbenes are considered to be planar, **1c** should be lower in energy. The observed temperature-dependent isomerization between triplet carbenes (**2c** → **1c**) is very unusual in that the more localized (as judged from the larger *D* value) carbene **1c** was found to be more stable, whereas the stability of radicals in general is thought to be increased with greater π-conjugation. MP2 calculations find **1c** to be lower in energy by 1.41 kcal/mol. However, despite the agreement between theory and experiment, it remains difficult to rationalize the greater stability of **1c** by qualitative arguments.

Conclusion

These carbenes are analogs of 2-propynylidene, and it was expected that the energy barrier between the two isomeric carbenes **1c** and **2c** would be very small, as reported in the 2-propynylidene interconversion.[9b] Therefore, the rearrangement (**1c** → **2c**) took place readily even at cryogenic temperatures. Our experimental results are summarized in Scheme 7. The carbene–carbene rearrangement takes place in two stages, right after photolysis of the diazo compounds and after annealing of the organic matrices.

By the irradiation of each diazo compound **1d** and **2d**, the corresponding carbenes **1c** and **2c**, respectively, were the primary products generated in EPR experiments, while carbene **2c** was the main product in the IR ones. How can we explain the apparently conflicting observations obtained from IR and EPR experiments? In these two kinds of experiments, the biggest point of difference is the use of different media, MTHF, isopentane, and EtOH-d_6 for EPR, Ar or isopentane for IR, and N_2 for UV–visible experiments. They could play an important role for the determination of the formation ratio during photolysis of the diazo compounds. Four states for each carbene were considered, and a plausible pathway from diazo compound to carbene is described in Scheme 8.

The photolysis of a diazo compound is an exothermic reaction[20] and generates the hot singlet carbene containing excess thermal

(19) Baird, N. C.; Taylor, K. F. *J. Am. Chem. Soc.* **1978**, *100*, 1333. Mueller, P. H.; Rondan, N. G.; Houk, K. N.; Harison J. F.; Hooper, D.; Willen, B. H.; Libman, J. F. *J. Am. Chem. Soc.* **1981**, *103*, 5049. Irikura, K. K.; Goddard, W. A., III; Beauchamp, J. L. *J. Am. Chem. Soc.* **1992**, *114*, 48. Russo, N.; Sicilla, E.; Toscano, M. *J. Chem. Phys.* **1992**, *97*, 5031.

(20) West, P. R.; Chapman, O. L.; LeRoux, J.-P. *J. Am. Chem. Soc.* **1982**, *104*, 1779. Simon, J. D.; Peters, K. S. *J. Am. Chem. Soc.* **1983**, *105*, 5156.

Scheme 7

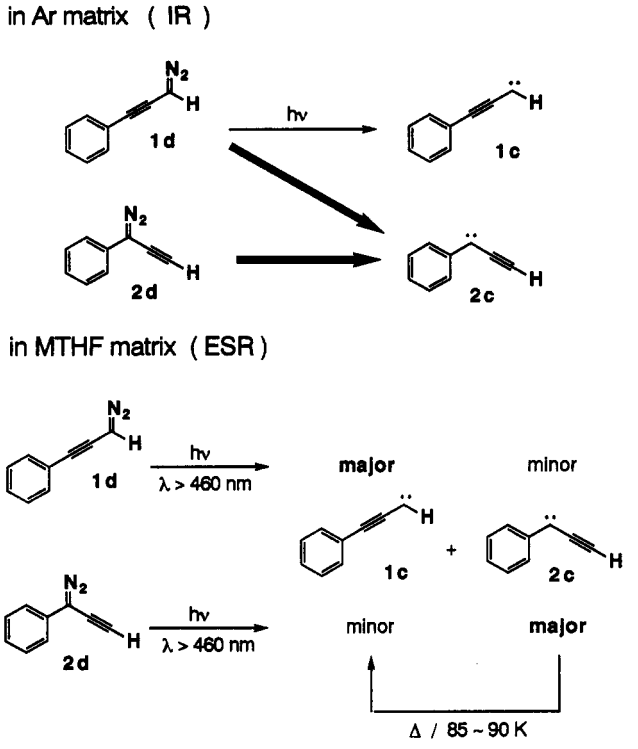

energy in the excited state. In an organic matrix such as MTHF, its excess energy is released into the medium, and it relaxes to the ground state before the rearrangement takes place. Therefore, the formation ratio (**1c**/**2c**) depends on the starting diazo compound. In an inert gas medium such as Ar, the excess thermal energy is used for overcoming the barrier between singlet carbenes **1c** and **2c** in the photoexcited state, followed by relaxation to the ground state. The formation ratio of **2c** in an Ar matrix is bigger, indicating that the energy minimum of **2c** in an argon matrix is deeper than that of **1c** in the excited state. Although the rearrangement from **2c** to **1c** was not observed in IR or UV–visible experiments in argon or nitrogen matrices below 40 K, the EPR observation of the shift from **2c** to **1c** in MTHF or EtOH-d_6 matrix at ca. 90 K suggests that triplet carbene **1c** is more stable than **2c** in the ground state, as shown in Scheme 8. Ab initio calculations at the MP2/DZV(d) level support these findings (Figure 8). The temperature, 90 K, is not intrinsic to the rearrangement, but it is the one at which the triplet ground-state carbene begins to change conformation due to the increasing mobility of the medium. This argument was supported by the result that at 67 K in isopentane matrix, a similar EPR spectral change was observed for **1c** and **2c**, and also by the result that the analogous carbene **7c** showed a similar temperature behavior.

In conclusion, the carbene–carbene rearrangement of the phenylpropynylidenes is medium-controlled and takes place in two stages, at the singlet excited state and at the triplet ground state. Carbene **1c** is apparently more thermodynamically stable than **2c** in the triplet state, while the opposite situation holds for the excited singlet state. An energy barrier for the rearrangement from **2c** to **1c** might be estimated to be less than 67 K (<133 cal/mol).

Experimental Section

General Methods. EPR spectra were obtained on a Bruker ESP 300 X-band spectrometer equipped with a Hewlett-Packard 5350B microwave frequency counter and an Air Products LTD-3–110 liquid helium transfer system. Infrared spectra were recorded on a Hitachi I-5040 FT-IR spectrometer. This IR spectrometer was modified by attaching a second sample room with a detector and a mirror. By a flipping of the mirror, the light for observation was led to the second sample room and was used for IR experiment without moving the cold head–sample block before and after photolysis of the attached samples. Electronic absorption spectra were measured on a JASCO UVDEC-610C spectrophotometer. ^{1}H NMR spectra were measured on a JEOL GX-270 Fourier transform spectrometer using either $CDCl_3$ or benzene-d_6 as solvent and referenced to TMS. Elemental analyses were performed in the Analytical Center of this department. Gel permeation chromatography employed Nippon Analytical Industry LC-09. High-performance liquid chromatography used JASCO PU-980 and UV-970 equipped with a reverse-phase column (Cica-Merk LiChrospher 100 RP-18(e) 4 × 250 mm^2). Either a Ushio 500-W high-pressure mercury lamp or a 300-W xenon lamp was used as the light source, and sharp-cut or band-path colored glass filters were used for selecting the irradiating wavelengths.

Photoproducts Analysis. Nitrogen was bubbled through 1.3–1.5 mM solutions (10 mL) of the diazo compound **1d** or **2d** in ethanol. The solutions were photolyzed with stirring through a color filter ($\lambda > 460$ nm) at 20 °C. The photolysis was followed by HPLC. After 60 min, the reaction mixture was poured into 100 mL of water saturated with NaCl and extracted with three 30-mL portions of ether. The combined ether layer was dried over anhydrous Na_2SO_4, followed by careful distillation to give a yellow oil. The mixture was dissolved in $CDCl_3$ containing TMS, and the ^{1}H NMR spectrum was measured. The photoproduct ratio was calculated from the integrated value of the signals. For the photolysis at 77 K, a Pyrex cuvette (10ϕ × 300 mm) and a liquid nitrogen dewar which had quartz windows for irradiation were used. An ethanol solution of **1d** in a cuvette was degassed by three freeze–thaw cycles and irradiated in liquid nitrogen through the window of the dewar. After 10 min, the cuvette was picked out and then left at room temperature in the dark. These procedures were repeated six times. The workup and determination of product ratios were performed by the procedure mentioned above.

Matrix Isolation Spectroscopy. Matrix isolation experiments were performed by a standard technique[21] using a closed-cycle helium cryostat (Daikin Cryo Kelvin) and a vacuum line to introduce the matrix gas and sublimed samples. CsI and sapphire plates were attached to a copper window holder at the end of the cold head for IR and UV–visible spectral measurements. This cold head with sample window was surrounded by a radiation shield. It had two opposing holes which were slightly larger than the window holder. The rotatable vacuum shroud surrounding the radiation shield had two opposing KBr windows for spectroscopic observation, a quartz window for irradiation of the sample, and a deposition plate which enabled deposition of matrix gas and the sample. For UV–visible spectral measurements, a quartz plate was used in place of KBr as one of the outer windows. The temperature was measured by a thermocouple (Au/Fe–chromel) and controlled by a temperature controller (Scientific Instrument Inc., Series 5500).

Materials. Solvents diethyl ether, tetrahydrofuran, 2-methyltetrahydrofuran, benzene, and toluene used for the reactions and spectral measurements were all distilled under high-purity N_2 after being dried with sodium/benzophenone ketyl. Dichloromethane was distilled under high-purity N_2 after being dried with calcium hydride. All reactions were stirred under an atmosphere of high-purity N_2. Typical workup consisted of aqueous quenching and ether extraction. Anhydrous magnesium sulfate was used as the drying agent. Solvents were removed on a rotary evaporator unless otherwise stated.

3-Amino-3-phenylpropyne Hydrochloride (2s). Twenty-one grams (0.11 mol) of 3-bromo-3-phenylpropyne was added dropwise with stirring to 400 mL of dry liquid ammonia. The mixture was refluxed for 4 h and left overnight for evaporation of ammonia. A solution of the resulting oil in ether was added to cold 6 N HCl. The aqueous layer was washed with diethyl ether and evaporated to dryness. The crude salt was crystallized from ethanol to afford 2.6 g (14%) of **2s**: IR (KBr disk) 3254 (≡C—H), 2859, 2043, 2124 (C≡C) cm^{-1}, ^{1}H NMR of the free base (270 MHz, $CDCl_3$) δ 2.23 (d, J = 2.6 Hz, 1H), 3.9–6.9 (very br, 2H), 4.78 (d, J = 2.2 Hz, 1H), 7.27–7.40 (m, 3H), 7.52–7.55 (m, 2H).

3-Acetamido-3-phenylpropyne (2b). To a solution of 1.0 g of **2s** and 1 mL of triethylamine in 20 mL of CH_2Cl_2, was added 0.89 g of acetyl chloride in 5 mL of CH_2Cl_2 at 0–5 °C. The mixture was stirred for 1 h at room temperature. Recrystalization from ether/hexane gave colorless needles in 70% yield: IR (KBr disk) 3293 (≡C—H or N—H), 2114 (C≡C), 1651 (C=O) cm^{-1}; ^{1}H NMR (270 MHz, $CDCl_3$) δ 7.49–7.53 (m, 2H), 7.32–7.41 (m, 3H), 6.03 (dd, J = 2.2 Hz, J' = 8.4 Hz, 1H), 5.97 (br, 1H), 2.49 (d, J = 2.2 Hz, 1H), 2.02 (s, 3H). Anal. Calcd for $C_{11}H_{11}NO$: C, 76.28; H, 6.40; N, 8.09. Found: C, 76.03; H, 6.40; N, 8.04.

(21) McMahon, R. J.; Chapman, O. L.; Hayes, R. A.; Hess, T. C.; Krimmer, H.-P. *J. Am. Chem. Soc.* **1985**, *107*, 7597.

Scheme 8

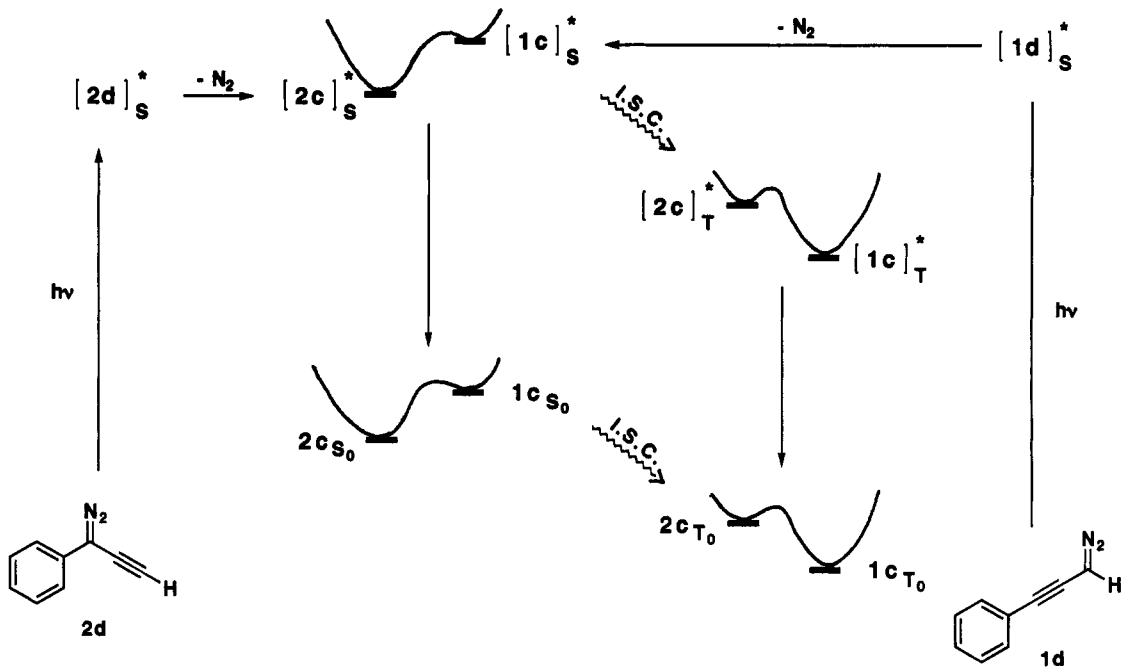

3-(*N*-Nitrosoacetamido)-3-phenylpropyne (2n). To a solution of 300 mg of **2b** in 5 mL of pyridine was added nitrosonium tetrafluoroborate in small portions with stirring under ice-cooling. At each addition, the reaction was monitored by silica gel TLC, and addition was continued until no **2b** was found by TLC. A pyridine solution was poured into water, followed by extraction with CH_2Cl_2. A yellowish green oil was obtained in quantitative yield: IR (NaCl) 3293 (≡C—H), 2130 (C≡C), 1732 (C=O), 1516 (-N=O) cm^{-1}; ^1H NMR (270 MHz, $CDCl_3$) δ 7.26–7.39 (m, 5H), 6.77 (d, J = 2.56 Hz, 1H), 2.80 (s, 3H), 2.48 (d, J = 2.57 Hz, 1H).

3-Diazo-3-phenylpropyne (2d). To an ether solution of nitrosoacetamido **2n** was added sodium hydroxide in ethyl alcohol dropwise at 5 °C, and the reaction was followed by Al_2O_3 TLC. An ether solution was washed by water, dried on sodium sulfate, and evaporated at room temperature. The crude diazo derivative was purified by aluminum oxide column chromatography (activity III) to afford a pink oil: IR (Ar matrix) 3321 (≡C—H), 2120 (C≡C), 2061 (C=N_2) cm^{-1}; ^1H NMR (270 MHz, C_6D_6) δ 7.10–7.14 (m, 2H), 6.92–7.02 (m, 3H), 3.63 (s, 1H); UV–visible (λ_{max}, pentane) 524, 280 nm.

3-Amino-1-phenylpropyne Hydrochloride (1s). Prepared according to a method reported in the literature:[22] IR (KBr disk) 2937, 2242 cm^{-1} (C≡C).

3-Acetamido-1-phenylpropyne (1b). This compound was prepared according to the procedure used for preparation of **2b**. A white powder was obtained after crystallization from EtOH: mp 78.2–79.4 °C; IR (KBr disk) 3301 (N—H), 1651 (C=O) cm^{-1}; ^1H NMR (270 MHz, $CDCl_3$) δ 7.40–7.43 (m, 2H), 7.28–7.33 (m, 3H), 5.74 (br,1H), 4.28 (d, J = 5.1 Hz, 2H), 2.03 (s, 3H). Anal. Calcd for $C_{11}H_{11}NO$: C, 76.28; H, 6.40; N, 8.09. Found: C, 76.03; H, 6.31; N, 8.23.

3-(*N*-Nitrosoacetamido)-1-phenylpropyne (1n). This compound was prepared using the same method used for preparation of **2n**. A yellow oil was obtained after silica gel column chromatography: IR (NaCl) 2256, 2221 (C≡C), 1736 (C=O), 1510 (-N=O) cm^{-1}; ^1H NMR (270 MHz, $CDCl_3$) δ 7.24–7.38 (m, 5H), 4.68 (s, 2H), 2.84 (s, 3H).

3-Diazo-1-phenylpropyne (1d). This compound was prepared by using the procedure employed for synthesis of **2d**. Analytically pure pink oil was obtained after aluminum oxide column chromatography: IR (Ar matrix) 3092, 2211 (C≡C), 2071 (C=N_2) cm^{-1}; ^1H NMR (270 MHz, C_6D_6) δ 7.41–7.46 (m, 2H), 7.00–7.11 (m, 3H), 3.76 (s, 1H); UV–visible (λ_{max}, pentane) 476, 296 nm.

3-Diazo-3-phenylpropyne-*1-d* (D1d). This compound was prepared from 1-phenyl-3,3-dideuterio-3-hydroxypropyne via six steps by using procedures similar to the ones used for preparation of **1d**. For alkali decomposition to diazo compound, $NaOCD_3$ was used. The obtained **D1d** was found to be deuterated by 80% from ^1H NMR spectrum: IR (Ar matrix) 2211 (C≡C), 2189 (≡C—H), 2071 (=N_2) cm^{-1}; ^1H NMR (270 MHz, acetone-d_6) δ 7.30 (m, 5H)

3-Phenylpropynal (1f).[23a] This compound was prepared according to the method described in the literature. A colorless oil was obtained by silica gel column chromatography (*n*-hexane:CH_2Cl_2 5–4:1 as eluents): IR (Ar matrix) 2870, 2858, 2247 (C≡C), 2203 (C≡C), 1672 (C=O) cm^{-1}; ^1H NMR (270 MHz, $CDCl_3$) δ 9.43 (s, 1H), 7.59–7.63 (m, 2H), 7.47–7.53 (m, 1H), 7.37–7.44 (m, 2H)

3-Phenylpropiolic Acid (1a). This compound was prepared according to a procedure in the literature.[23b] White needles were collected: IR (KBr disk) 3534 (O—H), 2251 (C≡C), 2229 (C≡C), 2222 (C≡C), 1738 (C=O) cm^{-1}; ^1H NMR (270 MHz, $CDCl_3$) δ 4.5–6.3 (very br, 1H), 7.36–7.43 (m, 2H), 7.45–7.52 (m, 1H), 7.63–7.60 (m, 2H).

Ethynyl phenyl ketone (2k): IR (KBr disk) 3311 (≡C—H), 2109 (C≡C), 1666 (C=O) cm^{-1}; ^1H NMR (270 MHz, $CDCl_3$) δ 3.44 (s, 1H), 7.47–7.54 (m, 2H), 7.61–7.67 (m, 1H), 8.18–8.19 (m, 2H).

Phenyl propiolate (7): IR (Ar matrix) 3307 (≡C—H), 2136 (C≡C), 1748 (C=O) cm^{-1}; ^1H NMR (270 MHz, $CDCl_3$) δ 3.07 (m, 1H), 7.12–7.17 (m, 2H), 7.24–7.31 (m, 1H), 7.37–7.45 (m, 2H).

3-Phenyl-3-ethoxypropyne (4). To a dry THF solution containing 2.14 mL of a hexane solution of *n*-butyllithium (1.6 M) were added at −25 °C 0.5 mL of a THF solution of 3-phenyl-3-hydroxyproppyne (0.43 g) and 1.2 mL of freshly distilled DMSO. After the solution was stirred at 0 °C for 5 min, 0.76 g of ethyl iodide was added. The mixture was stirred for 2 h at 0 °C and overnight at room temperature, poured into aqueous saturated ammonium chloride, and extracted with ether three times. The crude ether **4** was obtained in 82% yield (430 mg) and purified by GPC: ^1H NMR (270 MHz, $CDCl_3$) δ 1.26 (t, J = 6.96 Hz, 3H), 2.62 (d, J = 2.20 Hz, 1H), 3.56 (dq, J = 9.16 Hz, J' = 6.96 Hz, 1H), 3.75 (dq, J = 9.16 Hz, J' = 6.96 Hz, 1H), 5.16 (d, J = 2.20 Hz, 1H), 7.32–7.41 (m, 3H), 7.51–7.54 (m, 2H).

***trans*-1,6-Diphenyl-3-hexene-1,5-diyne (6).**[24] To a solution of 0.5 g (4.9 mmol) of phenylacetylene in 5 mL of THF was added dropwise at −77 °C 3.5 mL of 1.6 M hexane solution of *n*-butyllithium. After yellow precipitates were formed, 15 mL of a suspension of 0.67 g of zinc chloride in THF was added at 0–4 °C, and the mixture was stirred for 1 h at 3 °C. A suspension of 0.17 g of $[Pd(PPh_3)_2]Cl_2$, 0.49 mL of DIBAL, and 0.76 g of a *cis* and *trans* mixture of 1.2-dibromoethylene in 10 mL of THF was added to the metal-exchanged suspension. The cold bath was removed, and suspension was stirred for 60 h at room temperature and then for 90 min at the refluxing temperature. A reaction mixture was

(22) Klemm, L. H.; McGuire, T. M.; Gopinath, K. W. *J. Org. Chem.* **1976**, *41*, 2571.

(23) (a) Brandsma, L. In *Studies in Organic Chemistry 34. Preparative Acetylenic Chemistry*, 2nd ed.; Elsevier: Amsterdam, p 102. (b) Reference 23a, p 100.

(24) Carpita, A.; Rossi, R. *Tetrahedron Lett.* **1986**, *36*, 4351. Negishi, E.; King, A. O.; Okukado, N. *J. Org. Chem.* **1977**, *42*, 1821.

poured into 80 mL of water saturated by ammonium chloride and extracted with 100 mL of *n*-pentane three times. The combined *n*-pentane solution was washed by water three times and dried over magnesium sulfate. After evaporation of *n*-pentane, crude enediyne was purified by silica gel column chromatography (*n*-hexane as an eluent) and crystallization from *n*-hexane. Yellow needles (40 mg) were obtained in 7% yield: mp 110–112 °C; IR (KBr) 2203 (C≡C) cm^{-1}; ^1H NMR (270 MHz, $CDCl_3$) δ 6.29 (s, 2H), 7.31–7.36 (m, 6H), 7.43–7.50 (m, 4H); mass m/z = 228.

Computational Methodology. The geometries of the lowest triplet states of **1c** and **2c** were optimized by using an unrestricted Hartree–Fock wave function (UHF), while the lowest singlet-state geometries were optimized by a two-configuration generalized valence bond (GVB) wave function. All geometries were held planar during optimization. While geometry optimization at a correlated level would be preferable, such calculations were considerably more expensive and were therefore not attempted. The basis set used for geometry optimization was Dunning's [4s2p/2s] contraction[12] of Huzinaga's primitive (9s5p/4s) set.[25] Single-point energies were calculated by second-order perturbation theory (Møller–Plesset, MP2)[26] employing the DZ basis previously mentioned. In order to test the effect of polarization functions on the correlated total energies, the split valence contraction [3s2p/2s] of the DZ basis augmented by a set of five pure angular momentum d functions (α(d) = 0.75) on carbon (DZV(d)) was also used at the MP2 level.[13] The UHF wave functions were contaminated by states of higher multiplicity, as shown by the large values of the $\langle S^2 \rangle$ operator ($\langle S^2 \rangle$ = 3.182 and 3.164 at the UHF/DZ geometries for **1c** and **2c**, respectively). Projection of the first spin contaminant led to lower energies (not reported) and reduced ΔE(**1c**–**2c**) to 0.25 from 0.99 kcal/mol at the MP2/DZ level. Since a full spin projection of the UHF wave function was not carried out, the reliability of the UMP2 or PMP2 energies for comparing the relative stability of each isomer seems questionable. Thus, restricted open-shell MP2 theory (ROMP2) was also employed to compute the energies of the lowest triplet states at the UHF geometry. Because of the computational expense, only ROMP2 calculations were performed using the DZV(d) basis set on the triplet state. All geometry optimizations were performed using Gaussian 88[27] while the MP2 calculations were carried out using Gaussian 92.[28]

Acknowledgment. This work was supported by a Grant-in-Aid for Specially Promoted Research (No. 03102003) from the Ministry of Education, Science and Culture of Japan and by a grant for a postdoctoral fellowship to A.S.I. from the Japan Society for the Promotion of Science. Acknowledgment is made to the Institute for Molecular Science for a generous grant of computer time and to Prof. Lahti of University of Massachusetts for making his computational resources available to us.

(25) Huzinaga, S. *J. Chem. Phys.* **1965**, *42*, 1293.

(26) Møller, C.; Plesset, M. S. *Phys. Rev.* **1934**, *46*, 618. Binkley, J. S.; Gordon, S. S.; Pople, J. A. *Int. J. Quantum Chem.* **1975**, *9S*, 229.

(27) Frisch, M. J.; Head-Gordon, M.; Trucks, G. W.; Foresman, J. B.; Schlegel, H. B.; Raghavachari, K.; Robb, M. A.; Binkley, J. S.; Gonzalez, C.; Defrees, D. J.; Fox, D. J.; Whiteside, R. A.; Seeger, R.; Melius, C. F.; Baker, J.; Martin, R. L.; Kahn, L. R.; Stewart, J. J. P.; Topiol, S.; Pople, J. A. *Gaussian 90*; Gaussian Inc.: Pittsburgh, PA, 1990.

(28) Frisch, M. J.; Trucks, G. W.; Head-Gordon, M.; Gill, P. M. W.; Wong, M. W.; Foresman, J. B.; Johnson, B. G.; Schlegel, H. B.; Robb, M. A.; Replogle, E. S.; Gomberts, R.; Anfres, J. L.; Raghavachari, K.; Binkley, J. S.; Gonzalez, C.; Martin, R. L.; Fox, D. J.; Defrees, D. J.; Stewart, J. J. P.; Pople, J. A. *Gaussian 92*; Gaussian Inc.: Pittsburgh, PA, 1992.